Proceedings of the Korean Nuclear Autumn Meeting
Yongpyong, Korea, October 2003

The first tuning result of the PEFP RFQ

Ji-ho Jang, Yong-sub Cho, Kyoung-keun Jeong, Kyung-tae Sul,
Hyeok-jung Kwon, Young-jun Kim, and Jean-ho Na
Proton Engineering Frontier Project / KAERI
P.O.Box 105, YuSong, Daejon, Korea

Abstract

In this work, we present the first tuning result of the RFQ for the proton engineering frontier project (PEFP). We have adopted the TRASCO tuning method in oder to control the quadrupole and dipole field. After 4 tuning steps, we have got the dipole components to be less than ±2% of the quadrupole component.

1. Introduction

The PEFP RFQ cavity has been designed by the RFQ Design Codes[1]and constructed to accelerate proton beam from 50 keV to 3 MeV at the operating frequency of 350 MHz. The output emittances are 0.23 mm-mrad and 0.264 deg-MeV in the transverse and longitudinal directions. The beam transition rate is about 95.4%. The RFQ is a 4-vane type composed of 4 sections with 10 slug tuners for each quadrant. The basic drawing is given in Fig. 1. We have selected the vane voltage is varying from 70 kV to 100 kV mostly in the second section.

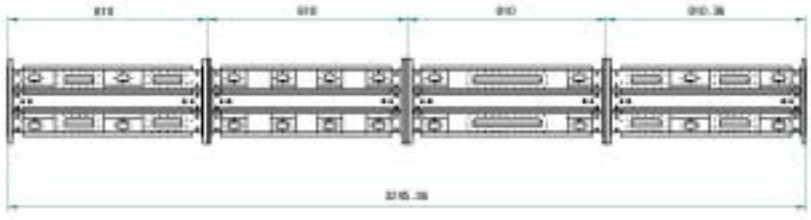

Figure 1. Basic drawing of PEFP RFQ.

An RFQ cavity can approximate to a wave-guide with end region satisfied with proper boundary conditions. We know that the under-cut in the end region is essential to satisfy the resonant frequency in a compact RFQ structure [2]. The length between vane and end-plate plays minor role than the under-cut because the magnetic field strength reduces rapidly as it's going away from the vane end.

In our RFQ, a coupling plate is used between the second and third sections for the mode stability. It is well known that the frequency difference between the operating mode (TE210) and the first excited mode becomes smaller for a longer cavity. That is a source of mode instability through the frequency perturbation. If we include the coupling plate, it's possible for the frequency of the nearest mode to move away from the operating mode. For example [3], the difference becomes 6.6 MHz after introducing the coupling plate from 1.9 MHz for a RFQ cavity with the length of 399.2 cm. Moreover, we can put two nearest modes equally separated from the operating mode and it enhances the mode stability.

There are four stabilization rods for the dipole mode control in the end plates and coupling plate in our RFQ cavity. The dipole stabilization rod for PEFP RFQ is long cylinder type which placed perpendicularly to the end palates and coupling plate. The LC resonant circuit in the plane between the rod and the first tuner is affected not by the quadrupole mode but by dipole modes because of symmetry[4]. It's possible to minimize the dipole effect if the quadrupole frequency is located at the center between two nearest dipole frequencies by controlling the rods.

This work is the first report of the tuning result for the PEFP RFQ cavity. Currently, the first two sections of the RFQ has been tuned to check our tuning process. Full RFQ tuning will start shortly. Our purpose is to make the quadrupole filed to be flat and dipole field to be less than the one percent of the quadrupole field.

The contents of this report are as follows. The experimental method and the tuning algorithm are given in section 2 and 3. Section 4 includes the main result of the tuning. The final conclusion is presented in section 4.

2. Experimental method

We have used the 4 tuners for each quadrant. In the beginning, the two end plates placed at 10 mm apart from the end of RFQ vanes and the stabilization rods go into the RFQ about 60 mm. Figure 2 shows the equipment setting for tuning.

The undercut of the PEFP RFQ has the shape of rectangle with dimension of 48.3mm x 30mm with blending of R6 in the inner corner edges. The designed cross-sectional frequency is 350MHz with tuners flush. However, we have initially set the tuners at 5mm inward from the wall. In this case, the resonant frequency of the operating quadrupole mode is changed to about 351 MHz.

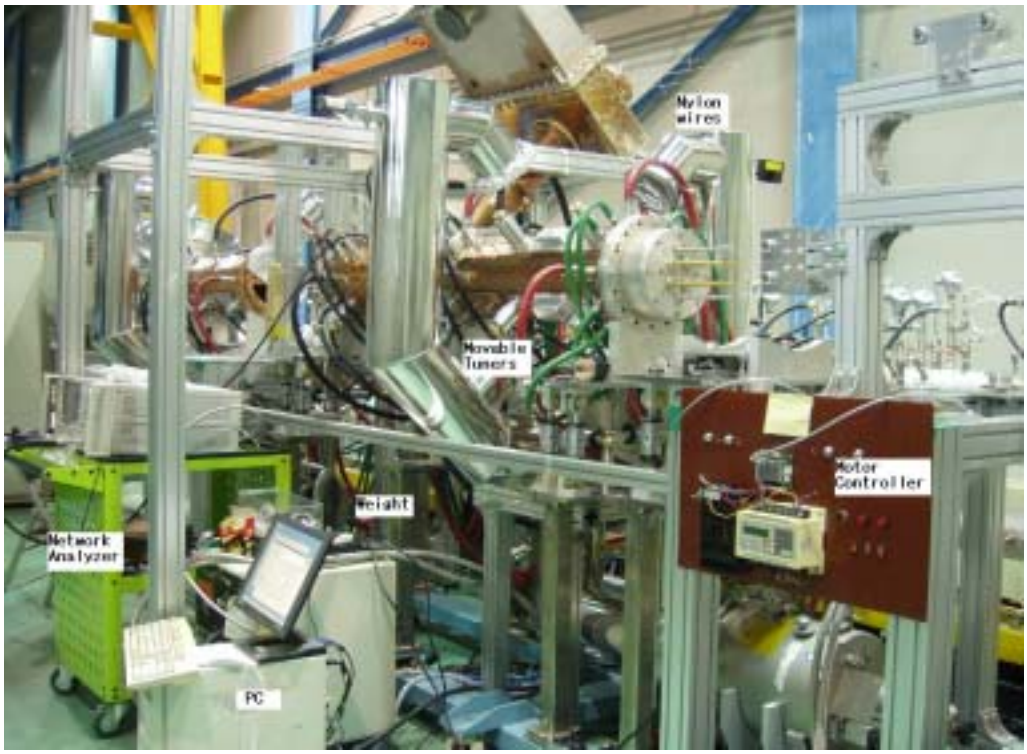

Figure 2. Bead test stand view.

We use aluminium beads of cylindrical shape with diameter 10mm and height 10mm. These beads are attached on four nylon wires running through the bisectors of each quadrant and 75mm from the center of the cavity (approximately 21mm from the walls, Figure 3). These nylon wires has diameter of approximately 0.85mm and strained by a 20kg weight. Stepping motors are used to pull the beads in constant speed of approximately 0.9mm/sec.

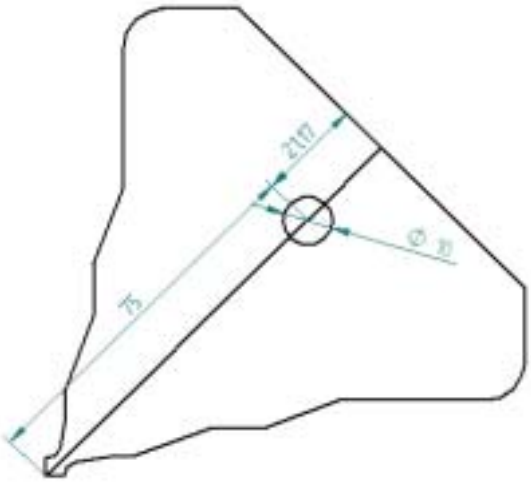

Figure 3. RFQ cross sectional view
and bead position.

An Agilent 8753ET/ES Network Analyzer is used to measure S11 amplitude values on every second. Due to the noises in amplitude signal we made additional processing in the raw data. Each trace value of a amplitude data are downloaded to a PC and fitted using square function in the vicinity of resonance point. Since we only need to find the symmetry point, square fitting (instead of more exact Lorentz distribution) is good enough for our purpose. We obtained less than 30Hz of statistical fluctuation in measured frequencies with fitting error less than 10Hz. This errors will be fine since the bead perturbation frequency shift is of order of a few kHz.

After measuring the field profile, the new tuner positions will be calculated using the algorithm described in Ref.[5]. This process will be repeated until we obtain the desired accuracy.

3. Tuning algorithm

This section includes the tuning algorithm to get the designed magnetic field pattern by the 4 slug tuners in each quadrant of the RFQ cavity. We have adopted the TRASCO tuning method[5].

Relation between quadrant fields and quadrupole/dipole field

The magnetic field in z-direction (beam direction) can be written by

$$B_Z(x,y,z,t) = F(x,y)\,V(z)\,T(t)$$

where $T(t) = e^{j\omega t}$ and we separate the field into two terms which depend on the transverse and longitudinal coordinates. If we concentrate on the z -dependant component, $V(z)$, we can define the quadrupole and dipole modes as follows,

$$V_1 + V_2 + V_3 + V_4 = 0,$$

$$V_Q = \frac{1}{4}(V_1 - V_2 + V_3 - V_4),$$

$$V_{D1} = \frac{1}{2}(V_1 - V_3),$$

$$V_{D2} = \frac{1}{2}(V_2 - V_4),$$

where V_Q, V_{D1}, and V_{D2} are the quadrupole and two dipole components, respectively. V_i is the magnetic field depending on z in the i-th quadrant. This formula can be replaced by the following form,

$$V_i = V_Q + V_D$$

$$V_D = \frac{1}{2}[(V_i + V_{i+1}) + (V_i + V_{i-1})]$$

where $i \pm 1 = i \pm 1 \mod 4$ and we have assumed that two dipole fields are degenerated in mode frequencies.

Wave equation for $B_Z(x,y,z,t)$

The magnetic field $B_Z(x,y,z,t)$ satisfies the following wave equation:

$$c^2 \nabla^2 B_Z - \frac{\partial^2 B_Z}{\partial t^2} = 0.$$

Since the spatial derivative of the field component $F(x,y)$ depending on the transverse coordinates can be replaced by the following relation:

$$c^2 \nabla_t^2 F(x,y) - \omega_i^2(z)\ F(x,y) = 0,$$

where $\omega_i(z)$ represents the resonant frequency of the cross section of the RFQ and it is varying function of z because of the manufacturing error. It's impossible to directly determine $\omega_i(z)$ by an experimental method. Using the above relation, we can obtain a wave equation for $V(z)$ as follows:

$$c^2 \frac{d^2 V_i(z)}{dz^2} + \left(\omega^2 - \omega_i^2(z)\right) V_i(z) = 0,$$

where ω is the frequency for each resonant mode. Since the quadrant fields is composed of the dipole and quadrupole fields, this equation becomes

$$c^2 \frac{d^2 V_i(z)}{dz^2} + (\omega_Q^2 - \omega_i^2(z))\, V_i(z) - (\omega_Q^2 - \omega_D^2)\, V_d(z) = 0,$$

where ω_Q and ω_d represent the quadrupole and dipole frequencies, respectively. If we use the fact that frequency difference is smaller than the quadrupole resonant frequency, $|\omega_Q - \omega_i(z)| \ll \omega_Q$, $|\omega_Q - \omega_d| \ll \omega_Q$, we can get the following result:

$$2\frac{\omega_Q - \omega_i(z)}{\omega_Q}\, V_i(z) + \left(\frac{\lambda_Q}{2\pi}\right)^2 \frac{d^2 V_i(z)}{dz^2} - \frac{\omega_Q - \omega_d}{\omega_Q}[(V_i(z) + V_{i+1}(z)) + (V_i(z) + V_{i-1}(z))] = 0,$$

where the second term is related with the quadrupole component and the third term represents the dipole perturbation.

Tuning Process

(1) We measure the quadrupole and dipole frequencies: ω_Q , ω_d.

(2) We measure the magnetic fields, $V_i(z)$, in each quadrant using the bead-pull method.

(3) After removing the bumps generated by the tuners and ports, we get fitting function for the data points of (2).

(4) We calculate the frequency shift, $\omega_i(z) - \omega_Q$, as a function of z by using the TRASCO formula.

(5) We change the tuner position in order to compensate the calculated frequency shift.

(6) We repeat the processes from (1) to (5).

4. Tuning result

Table 1 shows the frequency change when each tuner shifts from the wall to the 5 mm inward. From this table, we can obtain the desired tuner positions corresponding to the frequency shift by the result of tuning formula using the linear approximation.

Table 1. frequency shift in kHz under varying tuner position (5 mm inward from the wall).

	quadrant 1	quadrant 2	quadrant 3	quadrant 4
tuner 1	35.74	40.32	50.33	46.85
tuner 2	43.92	45.59	58.36	48.89
tuner 3	72.36	71.38	43.63	46.74
tuner 4	87.98	80.22	41.76	43.46

The tuners are initially placed at the position of 5 mm inward from the RFQ walls. The measured quadrants fields are given in figure 4. Figure 5 shows the quadrupole and dipole components.

We have repeated the tuning process four times in order to get the desired field pattern. In the last tuning step, we have measured again the relation between the tuner movement and the frequency shift in order to enhance the tuning accuracy. Table 2 includes the information about the frequency change for 2 mm shift of each tuner. We have also changed the experimental setup for the bead to be placed at more correct position in the last step.

Table 3 shows the frequency shift and tuner positions for each step.

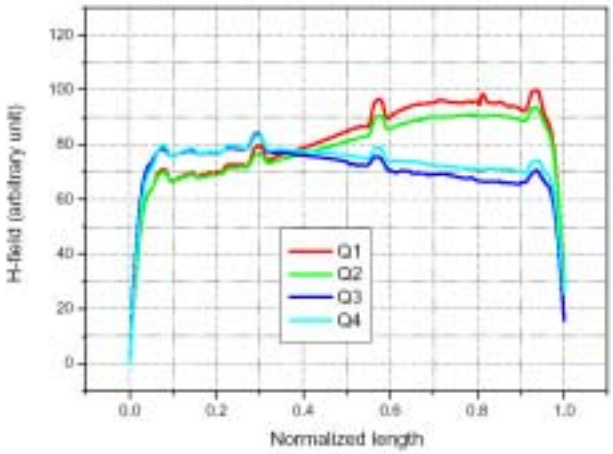

Figure 4. This initial magnetic field for each quadrant.

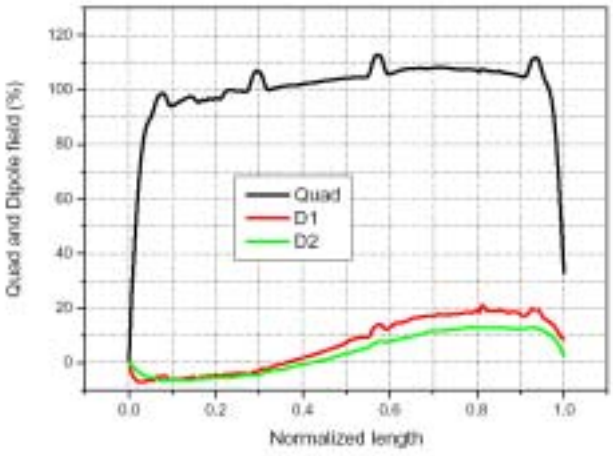

Figure 5. The initial quadrupole and magnetic fields.

Table 2. frequency shift in kHz under varying tuner position (2 mm inward from the tuner position after 2nd tuning)

	quadrant 1	quadrant 2	quadrant 3	quadrant 4
tuner 1	2.4	8.6	25.3	21.7
tuner 2	12.7	18.0	28.8	26.2
tuner 3	30.4	28.9	28.8	27.6
tuner 4	28.8	27.6	24.7	25.4

Table 3. Frequency shift and tuner position for each step of tuning process.

quadrant	tuner	1st tuning		2nd tuning		3rd tuning		4th tuning	
		δf (kHz)	position (mm)	δf (kHz)	position (mm)	δf (kHz)	position (mm)	δf (kHz)	position (mm)
1	1	-68.9	-4.6	-36.9	-9.8	-20	-12.6	-4.2	-16.1
	2	-42.0	0.2	-25.0	-2.6	-13.9	-4.2	-3.1	-4.7
	3	5.7	5.4	-0.93	5.3	-0.78	5.3	-0.5	5.6
	4	39.0	7.2	18.3	8.3	10.5	8.9	1.8	9.0
2	1	-55.7	-1.9	-24.8	-5.0	-15.1	-6.9	5.4	-5.7
	2	-34.5	1.2	-15.7	-0.5	-9.7	-1.6	3.5	-1.2
	3	5.0	5.4	3.2	5.6	1.7	5.7	-0.9	5.4
	4	34.0	7.1	18.8	8.3	11.6	9.0	-5.2	8.6
3	1	23.3	7.3	11.0	8.4	3.1	8.7	-7.3	8.1
	2	17.6	6.5	7.5	7.2	3.2	7.4	-5.1	7.0
	3	3.3	5.4	-0.9	5.3	3.5	5.7	-0.3	5.7
	4	-12.1	3.6	-9.2	2.4	3.7	2.9	4.2	3.2
4	1	13.8	6.5	13.9	8.0	1.2	8.1	-13.0	6.9
	2	10.0	6.0	11.8	7.2	1.6	7.4	-7.0	6.9
	3	0.1	5.0	6.9	5.7	2.5	6.0	5.7	6.4
	4	-8.4	4.0	2.2	4.3	3.4	4.7	16.6	6.0

The each quadrant and component (quadrupole and dipole) fields are shown in figures 6 and 7 after the first tuning, figures 8 and 9 after second tuning, figures 10 and 11 after the third tuning, and figures 12 and 13 after the last tuning.

We have found that the third tuning process does not give important modification. Since we have neglected the electric field effects when converting frequency change to the magnetic field, the result potentially include about 3 % error according to the result of the simulation using the SUPERFISH code[6] if the bead is positioned 5mm away from the exact position. That is why we have changed the experimental set up in the last step.

We also note that the quadrupole component is not changed significantly in each step and remains to be similar figure. However the dipole component becomes very small to be less than $\pm 2\%$. We note that there is some offset in the dipole component. The scale of dipole in figure 13 is 10 times larger than the measured value.

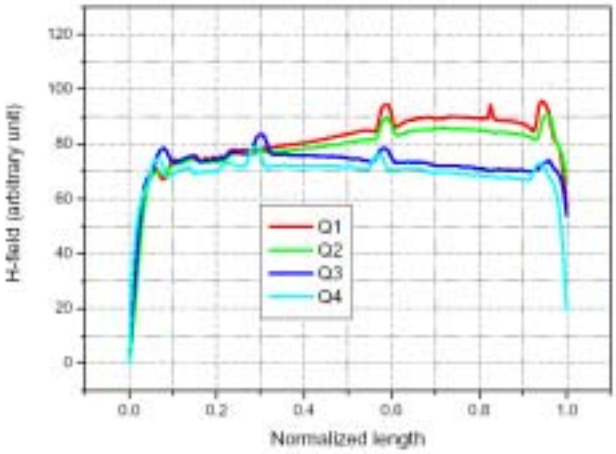

Figure 6. The magnetic fields for each quadrant after the first tuning process.

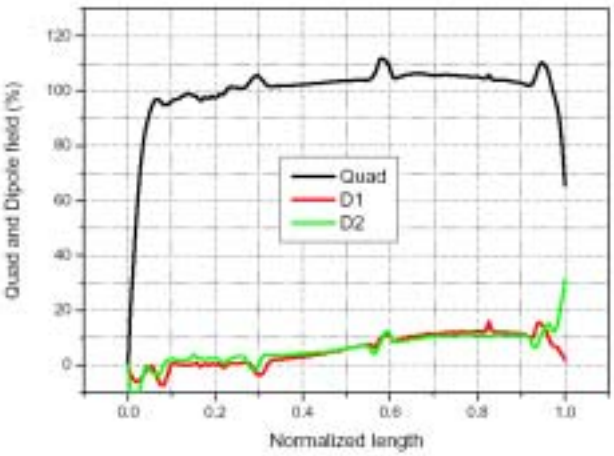

Figure 7. The quadrupole and dipole fields after the first tuning process.

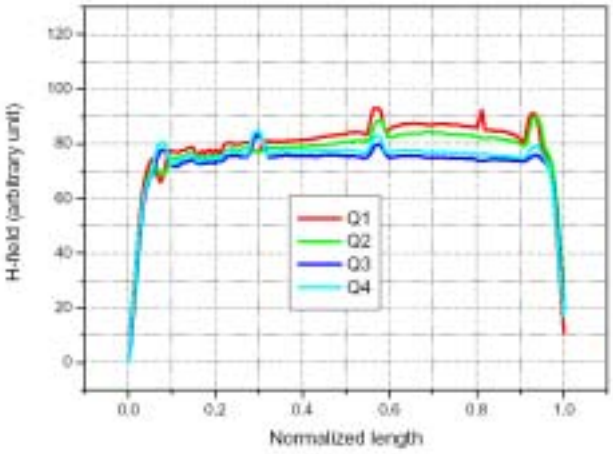

Figure 8. The magnetic fields for each quadrant after the second tuning process.

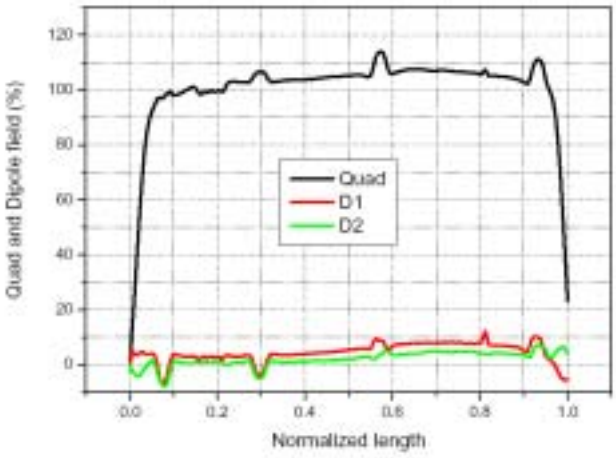

Figure 9. The quadrupole and dipole fields after the second tuning process.

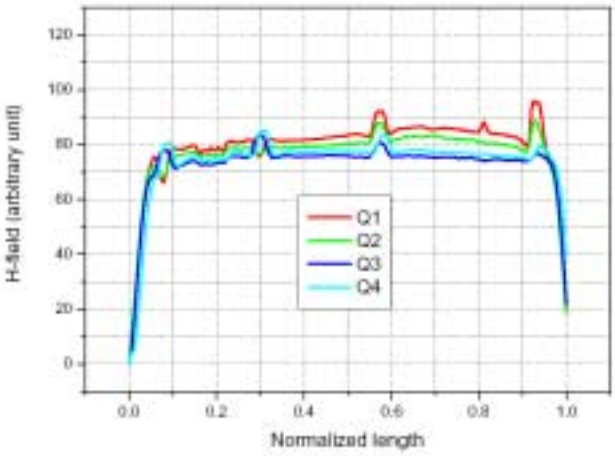

Figure 10. The magnetic fields for each quadrant after the third tuning process.

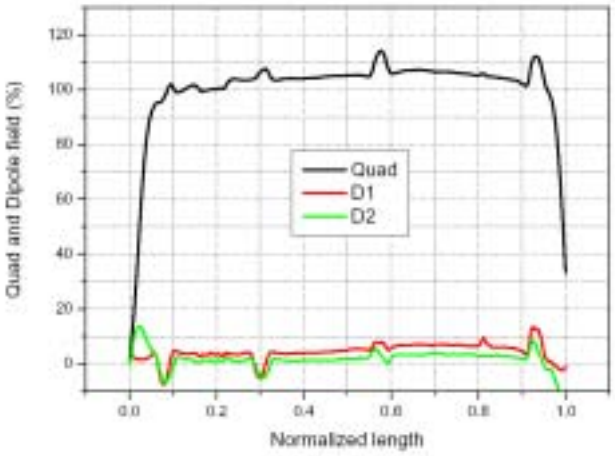

Figure 11. The magnetic fields for each quadrant after the third tuning process.

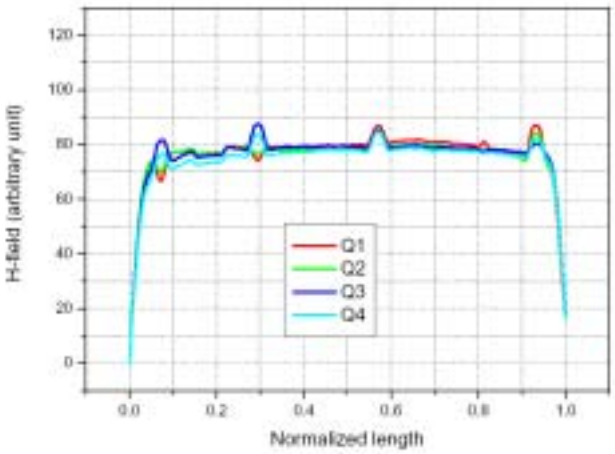

Figure 12. The magnetic fields for each quadrant after the fourth tuning process.

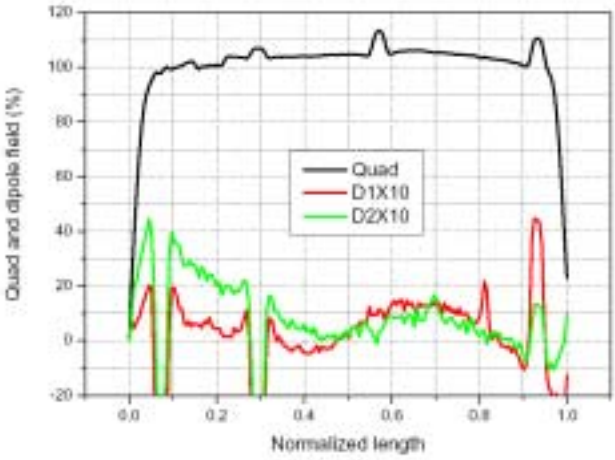

Figure 13. The quadrupole and dipole fields after the fourth tuning process.

5. Conclusion

In this work, we have checked the tuning process for the PEFP RFQ using the first two sections. The dipole mode is sufficiently suppressed within ±2% of the quadrupole mode after 4 tuning steps. However there remains some offset in the dipole mode and the quadrupole mode is not significantly modified in the tuning step. We have to resolve these problems.

The target field of the PEFP RFQ is not flat but increased mainly in the second section of the RFQ. That comes from the designed profile of the vane voltage and the geometrical change of each cross-section of the cavity. Hence the next step is to tune the cavity having the target field. And then, we will have to tune the full RFQ cavity with 4 sections separated into the 2 groups of 2 sections by the coupling plate.

6. References

1. RFQ Design Codes, LA-UR-96-1836, K. R. Crandall, et al.
2. Studying the End Regions of RFQs using the MAFIA codes, LINAC 88, M. J. Browman, G. Spalek, and T.C. Barts.
3. Coupled Radio-Frequency Quadrupoles as Compensated Stuctures, LINAC 90, M. J. Browman and L. M. Young.
4. Tuning and Stabilization of RFQ's, Linac 90, L. Young.
5. Field Tuning of the TRASCO RFQ, EPAC 2002, G.V. Lamanna, S. Fu, H.F. Ouyang, A. Palmieri.
6. POISSON/SUPERFISH, LA-UR-96-1824, J.H. Billen and L.M. Young.

ACKNOWLEDGEMENT

This work is supported by the 21C Frontier R&D program of MOST.